scientific reports

Check for updates

OPEN

Pomiferin protects against sepsis-associated acute liver and kidney injury via inhibition of NF-κB activation, oxidative stress, and cytochrome-c

Mohammad Alhilal[1✉], Huseyin Serkan Erol[2], Serkan Yildirim[3,4], Murat Koc[5], Suzan Alhilal[6], Esra Dereli[3], Tuba Karaarslan[7], Esra Aktas Senocak[8], Ilyas Bozkurt[9], Osman Nuri Keles[10] & Mesut Bunyami Halici[7]

In this study we report the first identification of the therapeutic effects of pomiferin isolated from *Maclura pomifera* against acute liver and kidney injury induced by sepsis. These results were obtained using a rat model of sepsis. We focused on targeting the nuclear factor kappa B (NF-κB) activation cascade, oxidative stress, and cytochrome-c, three key components involved in the pathophysiology of sepsis-associated acute liver and kidney injury. This assessment was conducted using biochemical, histopathological, immunohistochemical, and immunofluorescence analyses to examine parameters in liver and kidney tissues. The cecal ligation and puncture technique, used to induce sepsis, consistently caused acute liver and kidney damage. This was evidenced by significant increases ($p < 0.0001$), relative to untreated control rats, in the abundance of Toll-like receptor 4, NF-κB p65, phospho-NF-κB p65, 8-hydroxydeoxyguanosine, cytochrome-c, and caspase-3, higher degeneration, lipid peroxidation, and necrosis. This technique also caused significant decreases ($p < 0.001$) in components of the cellular antioxidant system in the hepatic and renal tissues of septic rats. Pomiferin, particularly at a dose of 300 mg/kg, showed promising pharmacological effects by reversing these pathological changes. Overall, pomiferin appears to protect liver and kidney tissues during sepsis by suppressing the NF-κB activation cascade, reducing oxidative stress, and lowering cytochrome-c activity. These effects suggest that pomiferin may be useful for managing sepsis patients with acute liver and kidney injury.

Keywords Pomiferin, Sepsis, Acute Liver and Kidney Injury, NF-κB activation, Oxidative stress, Cytochrome-c

Sepsis is a serious clinical condition[1] characterized by organ dysfunction resulting from an excessive immune response to infection[2]. Sepsis is linked to a high mortality rate across the world[3] and also places a substantial financial burden on the global health care sector[4]. The liver and kidney are the organs most affected, as the liver is the first to receive infection-derived components and products from the intestine via the portal circulation, and the kidneys filter large volumes of blood daily.

[1]Department of Nursing, Faculty of Health Sciences, Mardin Artuklu University, Mardin, Turkey. [2]Department of Biochemistry, Faculty of Veterinary Medicine, Balikesir University, Balikesir, Turkey. [3]Department of Pathology, Faculty of Veterinary Medicine, Ataturk University, Erzurum, Turkey. [4]Department of Pathology, Faculty of Veterinary Medicine, Kyrgyzstan-Turkey Manas University, Bishkek, Kyrgyzstan. [5]Department of Tradational, Complementary and Integrative Medicine, Public Health Institute, Ankara Yildirim Beyazit University, Ankara, Turkey. [6]Department of Medical Services and Techniques, Vocational School of Health Services, Mardin Artuklu University, Mardin, Turkey. [7]Department of Biochemistry, Faculty of Veterinary Medicine, Ataturk University, Erzurum, Turkey. [8]Department of Animal Science, Horasan Vocational College, Ataturk University, Erzurum, Turkey. [9]Department of Pharmacy Services, Nihat Delibalta Göle Vocational High School, Ardahan University, Ardahan, Turkey. [10]Department of Medical Histology and Embryology, Faculty of Medicine, Ataturk University, Erzurum, Turkey. ✉email: dr.mkh.1981@gmail.com; mohammadalhilal@artuklu.edu.tr

Acute liver injury and acute kidney injury are concerning pathological events that occur during sepsis. Sepsis-associated acute liver injury (SA-ALI) and sepsis-associated acute kidney injury (SA-AKI) disrupt many vital functions and thereby increase mortality rates[5,6]. It has been reported that 34%–46% of patients with sepsis develop liver dysfunction[7]. Sepsis is also linked to 25%–75% of acute kidney injury cases worldwide[8]. Despite advances in medical care and significant investment from the pharmaceutical industry, SA-ALI and SA-AKI remain major contributors to sepsis complications and mortality in affected patients.

Although the pathophysiology of SA-ALI and SA-AKI is not fully understood, several studies indicate that inflammation, oxidative stress, and apoptosis are key factors in their development[7,9–11]. The exaggerated inflammatory response is a major driver of pathological and biochemical abnormalities in the liver and kidneys during sepsis[12]. In addition to damaging cell components, reactive oxygen species (ROS) promote inflammation by activating the nuclear factor kappa B (NF-κB) pathway[13]. The progression of inflammatory events further increases oxidative stress, leading to tissue damage[14]. This interplay between inflammation and oxidative stress is a critical feature of sepsis pathophysiology[9], ultimately causing apoptosis and, consequently, organ failure. Targeting both inflammation and oxidative stress with anti-inflammatory and antioxidant agents is therefore an important therapeutic approach in SA-ALI and SA-AKI.

Recently, interest in isolated natural products with defined chemical structures has increased in medical research. Their popularity is due to the fact that some possess antioxidant and anti-inflammatory properties and do not appear to exert notable adverse effects. Pomiferin, a major isoflavone isolated from *Maclura pomifera* (Rafinesque) Schneider, a tree in the Moraceae family native to the United States and southeastern Canada[15], has shown promising therapeutic effects against gastric ulcer[16], acute respiratory distress syndrome[17], nickel-induced hepatic injury[18], and neurodegenerative diseases[19] by inhibiting oxidative stress and inflammation pathways. In addition, osajin, another isoflavone that has been isolated from *M. pomifera*, has shown protective effects against sepsis-induced liver[20] and kidney[21] damage. Based on these findings, we designed this study to evaluate the ability of pomiferin to reduce SA-ALI and SA-AKI by targeting the NF-κB activation series, oxidative stress, and cytochrome-c, which are key drivers of inflammation, cell damage, and apoptosis in these conditions. Experimental polymicrobial sepsis was induced in Sprague–Dawley rats via the cecal ligation and puncture (CLP) procedure, and biochemical, histopathological, immunohistochemical, and immunofluorescence techniques were used for evaluation.

Materials and methods

Plant material samples and isolation of pomiferin

The fruits of *Maclura pomifera* (Rafinesque) Schneider were collected from Ankara province, 845 m, around Atatürk Orman Çiftliği, 36 S 482,533 E—4,420,846 N, grassy levels in Türkiye during the flowering season in 2016. Identification and authentication of the plant material were conducted by Dr. Murat KOÇ, taxonomist, from Department of Traditional, Complementary and Integrative Medicine, Graduate School of Public Health, Ankara Yildirim Beyazit University, Türkiye. A voucher specimen of *M. pomifera* (Accession ID: Koç 3275) was deposited at the Herbarium of the Department of Traditional, Complementary and Integrative Medicine, Ankara Yildirim Beyazit University, Türkiye. Ethyl acetate (5 × 2.5 L) was used to extract the dried fruits of *M. pomifera* at room temperature. A rotary evaporator was used to remove the organic solvent, yielding a viscous yellow-green extract (114 g). Isoflavone pomiferin was then separated and purified using chromatographic methods, and its chemical structure, shown in Fig. 1, was confirmed by spectroscopic techniques (i.e., IR, 1D-NMR, and 2D-NMR). Comprehensive details of the extraction, isolation, and structural determination procedures have been described previously[16].

Animals and experimental model of sepsis

This study was approved by the Ethics Committee of Animal Experiments at Ataturk University, Erzurum, Turkey (Approval No. 134, Date. 01.09.2015). All experiments were performed in accordance with the relevant guidelines and regulations by this Committee. Moreover, this study was conducted in accordance with ARRIVE guidelines. Briefly, thirty adult male Sprague–Dawley rats were obtained from the Medical Experimental Application and Research Center at Ataturk University. Polymicrobial sepsis was then induced using the CLP technique, as previously described by Fujimura et al.[22]. To induce general anesthesia, fasted rats were injected intraperitoneally with thiopental sodium (25 mg/kg). After an abdominal incision was made, the following steps were performed to establish the sepsis model: retraction of the cecum through the peritoneum and muscles, ligation of the cecum with 4.0 silk suture, puncturing the ventral side of the cecum twice with an 18-gauge needle to facilitate the spread of feces into the peritoneum, returning the cecum and intestines, and closing the abdomen with 3.0 silk suture.

Experimental groups and description

Pomiferin doses were selected based on previous reports[16,23]. At high doses of pomiferin, death in animals, toxic effects, or pathological changes in different tissues were not reported[18,24]. Administration of pomiferin at doses (150, 200, or 300 mg/kg) demonstrated pharmacological effects against gastric ulcers, liver toxicity, and ovarian damage[16,18,25]. Ceftriaxone (CTX), an antibiotic commonly used to treat severe sepsis in intensive care units, was used as the standard drug. Figure 2 summarizes the applied procedures and experimental groups.

Twenty-four hours after the CLP procedure and surgery, all rats were euthanized by cervical dislocation under general anesthesia with thiopental sodium. The livers and kidneys were immediately excised, and biopsies were taken for biochemical, histopathological, immunohistochemical, and immunofluorescent analyses. For biochemical tests, liver and kidney tissues were stored at − 80 °C, while samples for histopathological, immunohistochemical, and immunofluorescent analyses were fixed in 10% formalin.

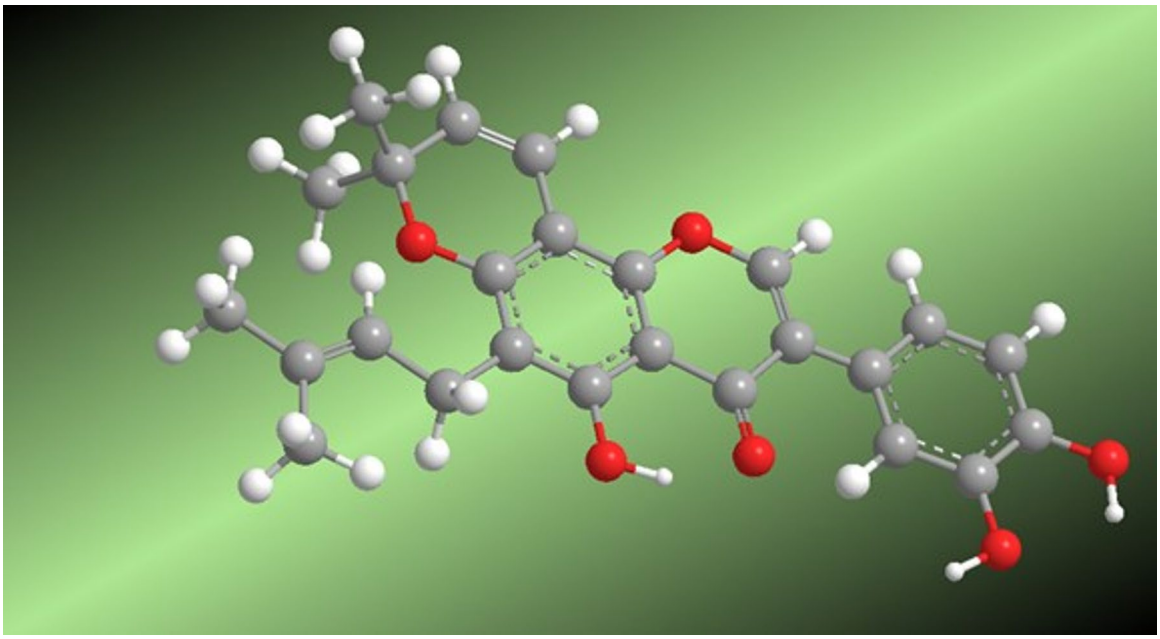

Fig. 1. The structure of pomiferin.

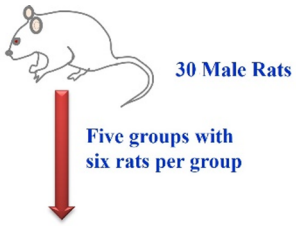

Group name	Description	Administration method (Pomiferin or CTX) /Time	Liver and kidney tissue collection time
Sham	Laparotomy without CLP	-	24 hours after the operation
CLP	CLP	-	24 hours after the CLP procedure
CLP+Pom150	150 mg/kg (BW) Pomiferin + CLP	Oral gavage/15 minutes before the CLP procedure	24 hours after the CLP procedure
CLP+Pom300	300 mg/kg (BW) Pomiferin + CLP	Oral gavage/15 minutes before the CLP procedure	24 hours after the CLP procedure
CLP+CTX	50 mg/kg (BW) CTX + CLP	Intraperitoneal injection/15 minutes before the CLP procedure	24 hours after the CLP procedure

Fig. 2. The applied procedures and experimental groups. BW: body weight, Ceftriaxone (CTX), CLP: cecal ligation and puncture, Pomiferin (Pom).

Preparation of liver and kidney tissues and biochemical tests

Frozen liver and kidney tissues were pulverized with liquid nitrogen using a tissue homogenizer. The following buffers were used for homogenization: lipid peroxidation (LPO), 10% KCl; glutathione (GSH), 50 mmol Tris–HCl pH 7.4; superoxide dismutase (SOD), 50 mmol KH_2PO_4, 10 mmol EDTA pH 7.8; and catalase (CAT), 50 mmol KH_2PO_4 pH 7. All homogenates were centrifuged at 4 °C in a refrigerated centrifuge, and the supernatants were collected for biochemical measurements using a Spectrophotometer Epoch. Details of the biochemical tests can be found in previous reports[20,21].

Key points are summarized below:

LPO determination
Malondialdehyde (MDA) levels were measured to assess LPO concentrations according to the method of Ohkawa et al.[26]. This method is based on the reaction of thiobarbituric acid with MDA to produce a red color, measured at 532 nm.

GSH determination
GSH concentrations were measured using the method of Sedlak and Lindsay[27], which detects a yellow color formed by the reaction of DTNB with sulfhydryl groups in GSH. This reaction is quantified by measurement at 412 nm.

SOD determination
SOD activity was measured according to the protocol of Sun et al.[28]. This method is based on the ability of SOD to inhibit formazan dye formation from NBT, with absorbance measured at 560 nm.

CAT determination
CAT activity was measured according to the protocol of Aebi[29], which is based on quantifying the decrease in absorbance at 240 nm caused by the conversion of hydrogen peroxide to water by CAT.

Biochemical tests in serum
Sera were collected to detect the levels of urea and creatinine. Detection kits from ELBA were used to measure these biochemical parameters with a spectrophotometer and data was evaluated with GEN 5 software.

Histopathological study of liver and kidney tissues
Liver and kidney tissues collected for histopathological evaluation were fixed in 10% formalin solution for 48 h, then washed with running tap water for 10 h. After passing through an alcohol and xylol series, the samples were embedded in paraffin blocks. Section 4 µm thick were cut from each block, stained with hematoxylin-eosin (H&E), examined under a light microscope (Leica DM 1000, Germany), and photographed.

Immunohistochemical study of liver and kidney tissues
Sections mounted on adhesion (poly-L-lysin) slides were processed before antibody incubation by passing through xylol and alcohol gradients, treating with 3% hydrogen peroxide for 10 min to block endogenous peroxidase activity, and applying antigen retrieval solution in a microwave oven, followed by cooling. The tissues were then incubated with primary antibodies, Toll-like receptor 4 (TLR4) and NF-κB p65 (Cat no: ab22048, Cat no: ab16502, diluted 1/100), at 37 °C for 60 min. Immunohistochemistry was performed according to the manufacturer's protocol (Abcam HRP/DAB Detection IHC kit). 3,3′-Diaminobenzidine (DAB) was used as the chromogen, and hematoxylin was used for background staining. Stained sections were evaluated using a light microscope (Zeiss AXIO, Germany).

Double immunofluorescent study of liver and kidney tissues
Following the procedures described previously[21], histological sections mounted on adhesion (poly-L-lysin) slides were incubated with primary antibodies, cytochrome-c (Cat No: ab150422) and 8-hydroxydeoxyguanosine (8-OHdG) (Cat No: sc66036), diluted 1/100. The secondary antibody (FITC, Cat No: ab6785, diluted 1/1000) was applied, and samples were incubated in darkness for 45 min. The same procedure was applied to sections using phospho-NF-κB p65 (p-NF-κB p65) and caspase-3 (Cat No: ab264271, Cat No: sc56053, diluted 1/100) as second primary antibodies, and Texas Red (Cat No: ab6719, diluted 1/1000) as the secondary antibody. DAPI with mounting medium (Cat No: D1306, diluted 1/200) was added to the sections and kept in darkness for 5 min. Sections were evaluated under a fluorescence microscope (Zeiss AXIO, Germany).

Statistical analyses
All statistical analyses were performed using GraphPad Prism version 8.0.2. A p value < 0.05 was considered as the threshold of statistical significance. For biochemical results, Kolmogorov–Smirnov tests were used to assess the normality of data distribution. Next, one-way ANOVAs followed by Tukey's tests were used to determine the statistical significance of differences between group means. For histopathological results, Duncan's test was used for inter-group comparisons. The nonparametric Kruskal–Wallis test and the Mann–Whitney U test were utilized to detect group interaction and differences between groups, respectively. To determine the intensity of positive staining from images obtained by immunohistochemical and immunofluorescence staining, 5 randomly selected areas were chosen from each sample and evaluated using ZEISS Zen Imaging Software. Data were statistically described as mean ± SD for the percentage of areas. One-way ANOVA followed by Tukey's test was performed to compare immunoreactive cells and immunopositive stained areas with healthy controls.

Results
Biochemical examination of oxidative stress parameters in the liver and kidney tissue
LPO
The results of measured LPO levels in the liver and kidney are shown in Figs. 3 and 4, respectively. Significant increases ($p < 0.0001$) were observed in the CLP group relative to the Sham group. Pomiferin administration suppressed these increases, with the strongest therapeutic effects observed at 300 mg/kg in the CLP+Pom300 group for hepatic tissues.

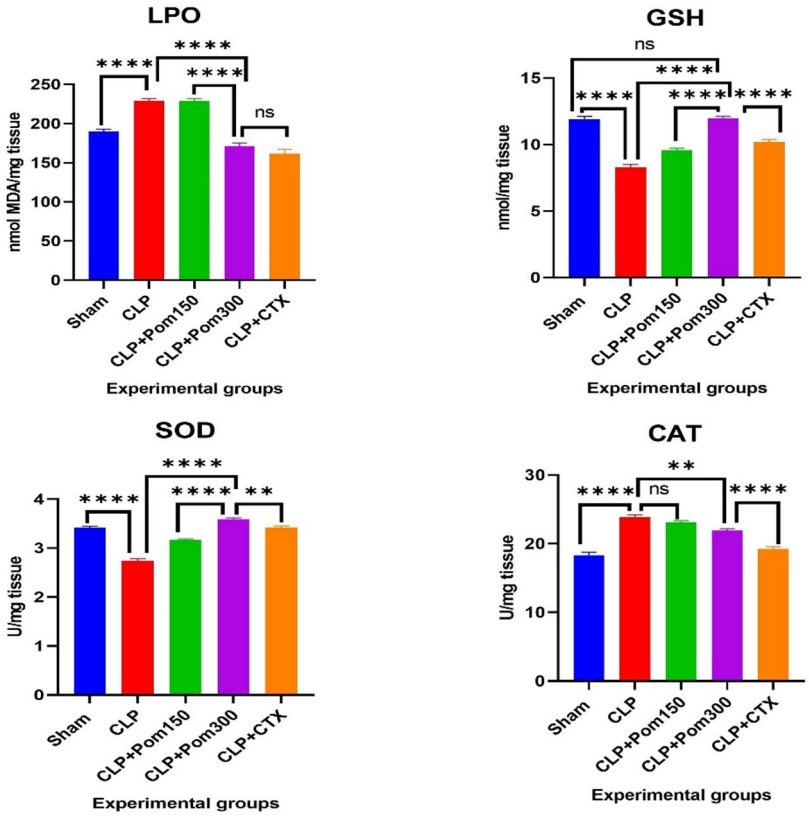

Fig. 3. Effect of pomiferin and CLP technique on oxidative stress parameters in liver tissues. CLP: Cecal ligation and puncture, Pom: Pomiferin, CTX: Ceftriaxone. Findings are expressed as mean ± SE. ****($p < 0.0001$). ** (for SOD $p = 0.0066$; for CAT $p = 0.0052$). ns: Nonsignificant difference (for LPO $p = 0.3831$; for GSH $p = 0.9994$; for CAT $p = 0.5211$).

GSH

The results of measured GSH levels in the liver and kidney are shown in Figs. 3 and 4, respectively. Significant decreases in GSH levels in liver ($p < 0.0001$) and kidney ($p = 0.0006$) tissues were observed in the CLP group compared to the Sham group. In contrast, pomiferin attenuated this decline relative to the CLP group. Administration of pomiferin at 300 mg/kg produced a higher increase in GSH for the CLP+Pom300 group than for the CLP+Pom150 or CLP + CTX groups ($p < 0.0001$).

SOD

SOD activity results in the liver and kidney are shown in Figs. 3 and 4, respectively. Significant decreases ($p < 0.0001$) were found in the CLP group compared to the Sham group. Conversely, pomiferin inhibited this decline. Administration at 300 mg/kg resulted in a greater increase for the CLP+Pom300 group than for the CLP+Pom150 ($p < 0.0001$) or CLP + CTX ($p = 0.0066$) groups in liver tissue. This was also true when compared to CLP+Pom150 ($p = 0.0014$) and CLP + CTX ($p = 0.0471$) in kidney tissue.

CAT

CAT activity results for the liver and kidney are shown in Figs. 3 and 4, respectively. In hepatic tissue, a significant increase ($p < 0.0001$) was observed in the CLP group compared to the Sham group, whereas in renal tissue, a significant decrease ($p = 0.0006$) was found. Pomiferin at 300 mg/kg produced the greatest increases in renal CAT activity for the CLP+Pom300 group, and also caused a significant increase ($p < 0.0001$) in hepatic CAT activity compared to the CLP + CTX group.

Biochemical examination of urea and creatinine in serum

The results of measured urea and creatinine levels in the serum are shown in Fig. 5. Significant increases ($p < 0.001$) were observed in the CLP group compared to the Sham group. Pomiferin application inhibited these increases, indicating the improvement of renal function.

Histopathological study of liver and kidney tissues

We characterized the results per treatment as follows

1. Sham: Normal liver (Fig. 6) and kidney (Fig. 7) structures were observed in this group.

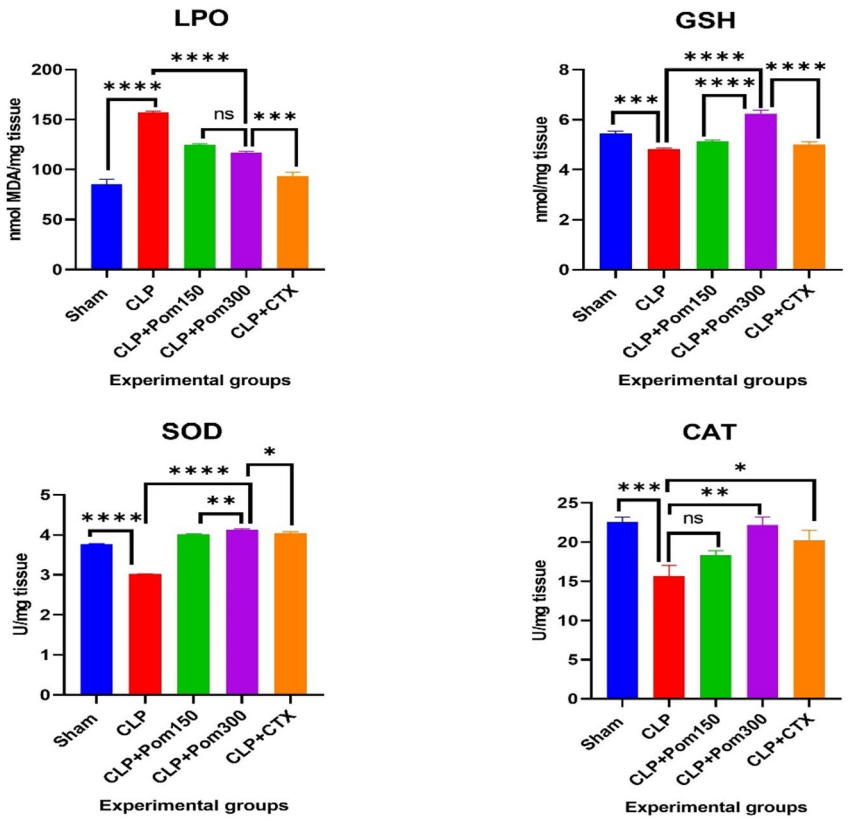

Fig. 4. Effect of pomiferin and CLP technique on oxidative stress parameters in kidney tissues. CLP: Cecal ligation and puncture, Pom: Pomiferin, CTX: Ceftriaxone. Findings are expressed as mean ± SE. **** ($p < 0.0001$). ***(for LPO $p = 0.0001$; for GSH and CAT $p = 0.0006$). ** (for SOD $p = 0.0014$; for CAT $p = 0.0011$). * (for SOD $p = 0.0471$; for CAT $p = 0.0293$). ns: Nonsignificant difference (for LPO $p = 0.4164$; for CAT $p = 0.3657$).

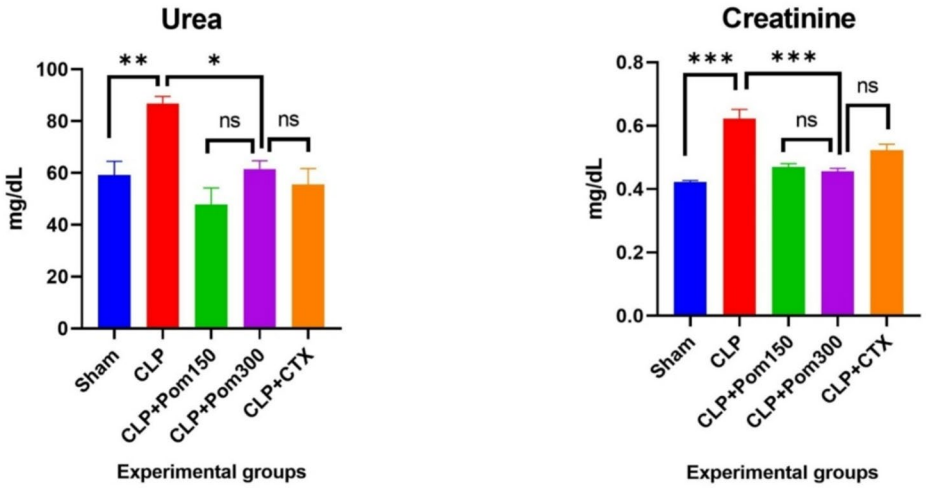

Fig. 5. Effect of pomiferin and CLP technique on urea and creatinine levels in serum. CLP: Cecal ligation and puncture, Pom: Pomiferin, CTX: Ceftriaxone. Findings are expressed as mean ± SE. *** ($p < 0.001$). ** ($p = 0.005$). * ($p = 0.011$). ns: Nonsignificant difference ($p > 0.05$).

2. CLP: In the liver, severe degeneration and necrosis of hepatocytes in the acinar region, along with hyperemia in the sinusoidal and interstitial vessels, were observed (Fig. 6). In the kidney, interstitial nephritis and severe degeneration and necrosis of the tubular epithelial cells were the main histopathological changes. Hyperemia was also present in the interstitial vessels (Fig. 7).

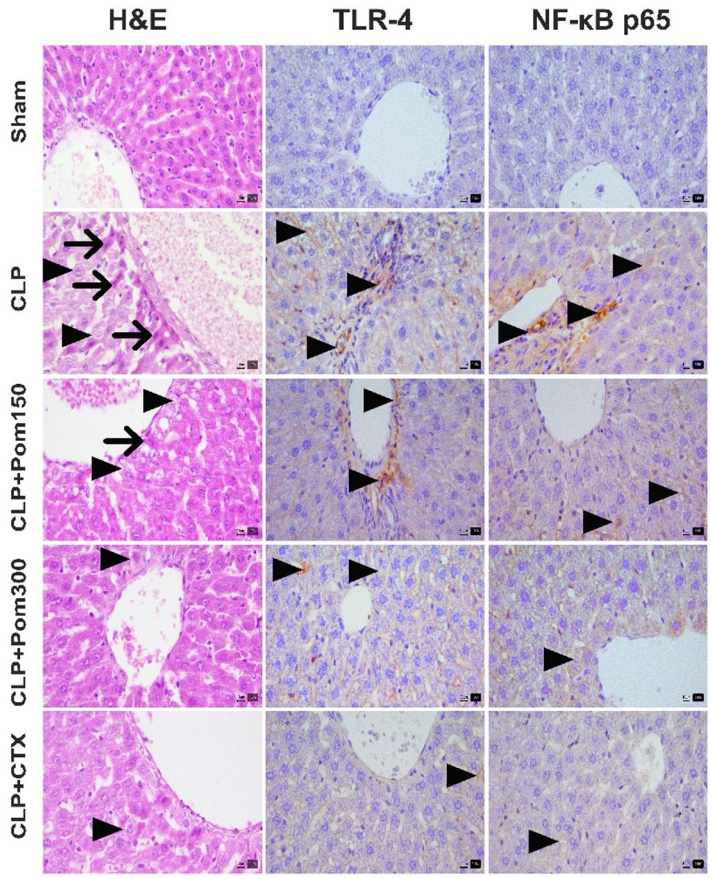

Fig. 6. Images of histopathological and immunohistochemical examination of liver sections. H&E: Degeneration in hepatocytes (arrowheads), Necrosis (arrows). IHC-P: TLR-4 and NF-κB p65 expressions (arrowheads). CLP: Cecal ligation and puncture, Pom: Pomiferin, CTX: Ceftriaxone, TLR4: Toll-like receptor 4, NF-κB p65: Nuclear factor kappa B p65. H&E, Bar: 10 μm. IHC-P, Bar: 10 μm.

3. CLP+Pom150: In the liver, moderate degeneration and necrosis of hepatocytes were observed in the acinar region (Fig. 6). In the kidney, moderate degeneration and necrosis occurred in the tubular epithelial cells (Fig. 7).
4. CLP+Pom300: Administration of pomiferin at 300 mg/kg showed the strongest therapeutic effects, reducing hepatocyte degeneration from severe to mild (Fig. 6). A similar improvement was observed in kidney tubular epithelial cells (Fig. 7).
5. CLP + CTX: In the liver, mild degeneration of hepatocytes was observed in the acinar region, with hyperemia in the sinusoidal and interstitial vessels (Fig. 6). In the kidney, mild degeneration was present in the tubular epithelial cells (Fig. 7).

Statistical analysis of histopathological findings is presented in Figs. 8 and 9 for the liver and kidney, respectively.

Immunohistochemical analysis of liver and kidney tissue

We characterized the results per treatment as follows:

1. Sham: TLR4 and NF-κB p65 expression was negative in both liver (Fig. 6) and kidney (Fig. 7) tissues.
2. CLP: Severe expression of TLR4 and NF-κB p65 was detected in inflammatory cells and some hepatocytes (Fig. 6). In kidney tissue, severe expression was present in inflammatory cells, around vessels, and in some tubular epithelial cells (Fig. 7).
3. CLP+Pom150: Moderate expression of TLR4 and NF-κB p65 was observed around vessels, in inflammatory cells, and in some hepatocytes (Fig. 6). Similar moderate expression was observed in kidney tissue, in inflammatory cells, around vessels, and in some tubular epithelial cells (Fig. 7).
4. CLP+Pom300: Pomiferin at 300 mg/kg produced the most pronounced therapeutic effects, reducing TLR4 and NF-κB p65 expression from severe to mild in both liver (Fig. 6) and kidney tissues (Fig. 7).
5. CLP + CTX: In the liver, mild expression of TLR4 and NF-κB p65 was present around vessels, in inflammatory cells, and in some hepatocytes (Fig. 6). In the kidney, mild expression was also detected in inflammatory cells, around vessels, and in some tubular epithelial cells (Fig. 7).

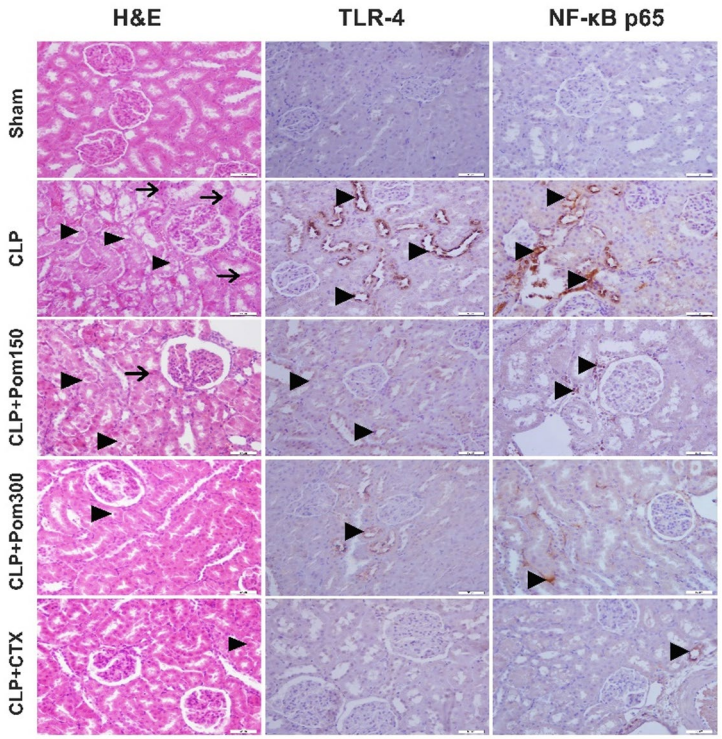

Fig. 7. Images of histopathological and immunohistochemical examination of kidney sections. H&E: Degeneration (arrowheads) and necrosis (arrows) in renal tubule epithelium. IHC-P: TLR-4 and NF-κB p65 expressions (arrowheads). CLP: Cecal ligation and puncture, Pom: Pomiferin, CTX: Ceftriaxone, TLR4: Toll-like receptor 4, NF-κB p65: Nuclear factor kappa B p65. H&E, Bar: 50 μm. IHC-P, Bar: 50 μm.

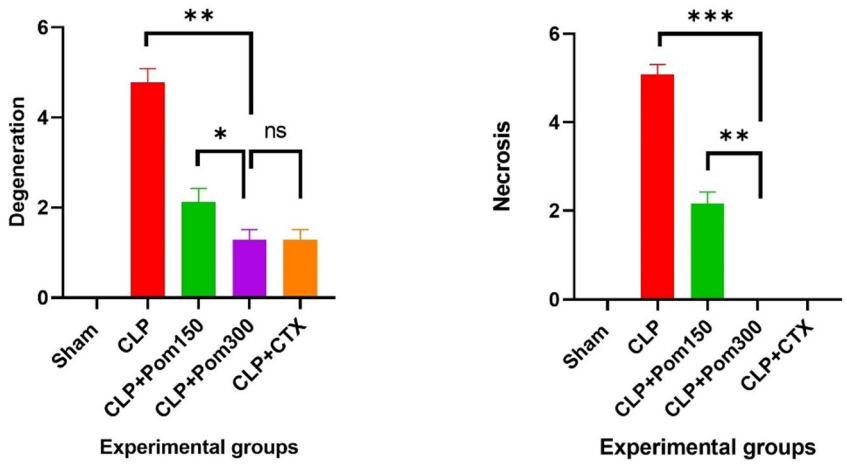

Fig. 8. Effect of pomiferin and CLP technique on degeneration and necrosis in liver tissues. CLP: Cecal ligation and puncture, Pom: Pomiferin, CTX: Ceftriaxone. Findings are expressed as mean ± SD. *** ($p < 0.0001$). ** ($p = 0.0022$). * ($p = 0.0159$). ns: Nonsignificant difference ($p < 0.05$).

Figures. 10 and 11 summarize the immunohistochemical results for liver and kidney tissues, respectively.

Double immunofluorescent study of liver and kidney tissue

We characterized the results per treatment as follows:

1. Sham: Cytochrome-c and p-NF-κB p65 expression was negative in liver (Fig. 12) and kidney (Fig. 13) tissues. Negative expression was also observed for 8-OHdG and caspase-3 in liver (Fig. 14) and kidney (Fig. 15) tissues.

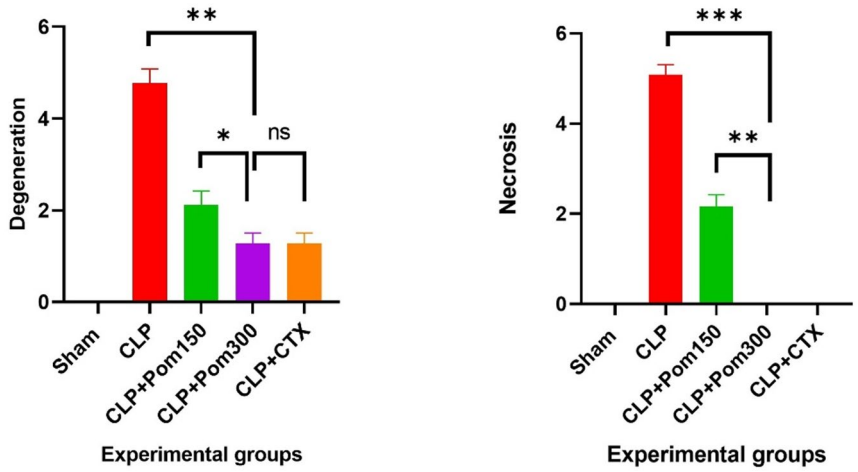

Fig. 9. Effect of pomiferin and CLP technique on degeneration and necrosis in kidney tissues. CLP: Cecal ligation and puncture, Pom: Pomiferin, CTX: Ceftriaxone. Findings are expressed as mean ± SD. *** ($p < 0.0001$). ** ($p = 0.0022$). * ($p = 0.0159$). ns: Nonsignificant difference ($p < 0.05$).

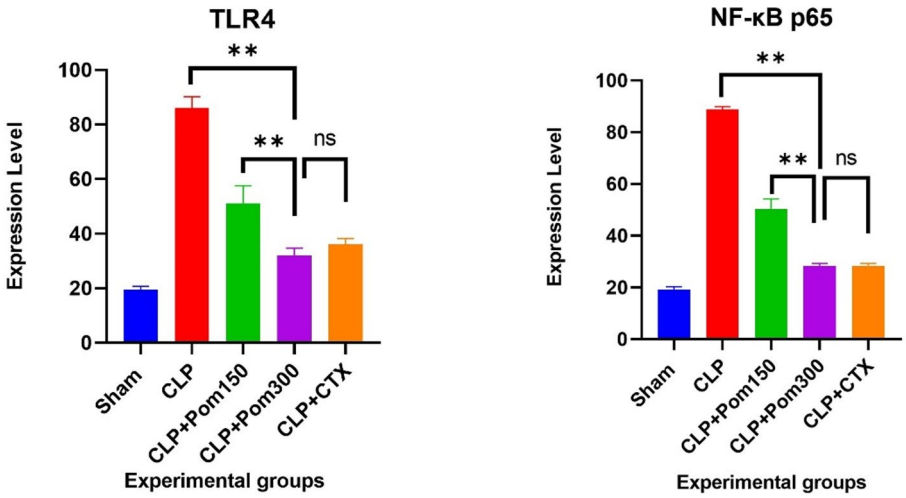

Fig. 10. Effect of pomiferin and CLP technique on TLR4 and NF-κB p65 expressions in liver tissues. CLP: Cecal ligation and puncture, Pom: Pomiferin, CTX: Ceftriaxone. Findings are expressed as mean ± SD. ** ($p = 0.0028$). ns: Nonsignificant difference ($p > 0.05$).

2. CLP: Severe expression of cytochrome-c and p-NF-κB p65 was observed in hepatocytes in the acinar region of the liver (Fig. 12) and in tubular epithelial cells of the kidney (Fig. 13). Severe expression was also present for 8-OHdG and caspase-3 in both liver (Fig. 14) and kidney (Fig. 15) tissues.
3. CLP+Pom150: Moderate expression of cytochrome-c and p-NF-κB p65 was observed in hepatocytes in the acinar region of the liver (Fig. 12) and in kidney tissue (Fig. 13). Moderate expression of 8-OHdG and caspase-3 was also seen in both liver (Fig. 14) and kidney (Fig. 15) tissues.
4. CLP+Pom300: Pomiferin at 300 mg/kg produced the most marked therapeutic effects, significantly reducing ($p = 0.0028$) cytochrome-c and p-NF-κB p65 expression compared to the CLP+Pom150 group in both liver (Fig. 12) and kidney (Fig. 13) tissues. Similar improvements were observed for 8-OHdG and caspase-3 in liver (Fig. 14) and kidney (Fig. 15) tissues.
5. CLP + CTX: Mild expressions of cytochrome-c and p-NF-κB p65 were determined in hepatocytes (Fig. 12) and in kidney (Fig. 13) tissue. These expressions also were mild for 8-OHdG and caspase-3 expressions in liver (Fig. 14) and kidney (Fig. 15) tissues.

Discussion

SA-ALI and SA-AKI remain major challenges in medicine despite significant advances in modern therapeutics and medical technologies. This is the first study to investigate the pharmacological potential of pomiferin against SA-ALI and SA-AKI. Our work targeted key cellular contributors to sepsis pathophysiology, including the NF-κB

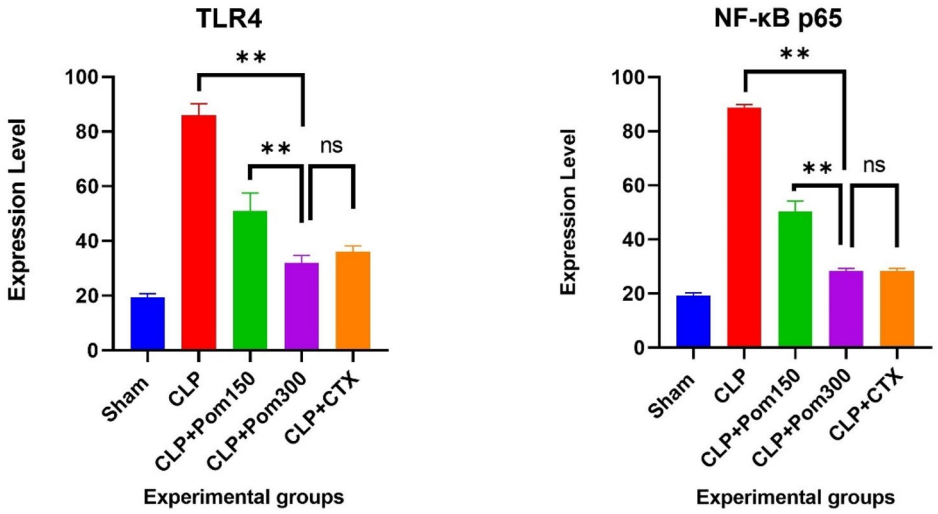

Fig. 11. Effect of pomiferin and CLP technique on TLR4 and NF-κB p65 expressions in kidney tissues. CLP: Cecal ligation and puncture, Pom: Pomiferin, CTX: Ceftriaxone. Findings are expressed as mean ± SD. **($p = 0.0028$). ns: Nonsignificant difference ($p > 0.05$).

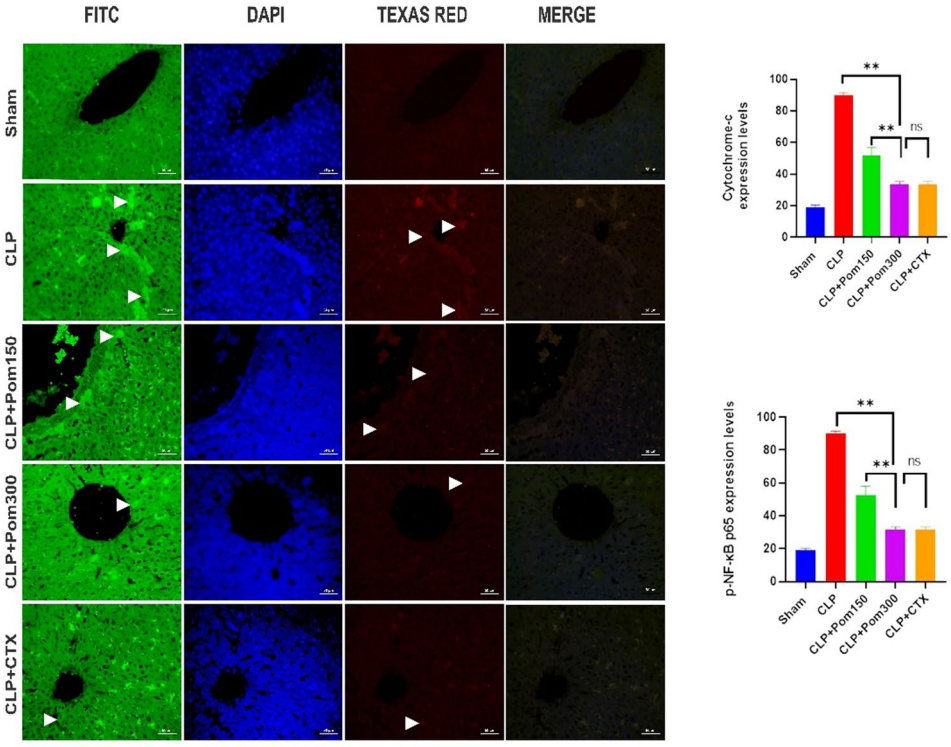

Fig. 12. Effect of pomiferin and CLP technique on cytochrome-c and p-NF-κB p65 expressions in liver tissues. Cytochrome-c expressions (arrowheads) (FITC); p-NF-κB p65 expressions (arrowheads) (TEXAS RED). CLP: Cecal ligation and puncture, Pom: Pomiferin, CTX: Ceftriaxone. Findings are expressed as mean ± SD. **($p = 0.0028$). ns: Nonsignificant difference ($p > 0.05$).

activation series, oxidative stress, and cytochrome-c. In the context of global efforts to find effective treatments for sepsis, we propose that pomiferin may represent a promising candidate and a novel therapeutic approach for managing sepsis patients. Inflammation is an essential defense against invading agents, but uncontrolled or systemic inflammation can lead to organ dysfunction, as occurs in sepsis[30]. In this study, inflammatory cytokines were not measured directly; instead, we examined the NF-κB activation series, which promotes nuclear NF-κB accumulation and upregulation of inflammatory cytokine gene transcription[31]. This cascade involves TLR4,

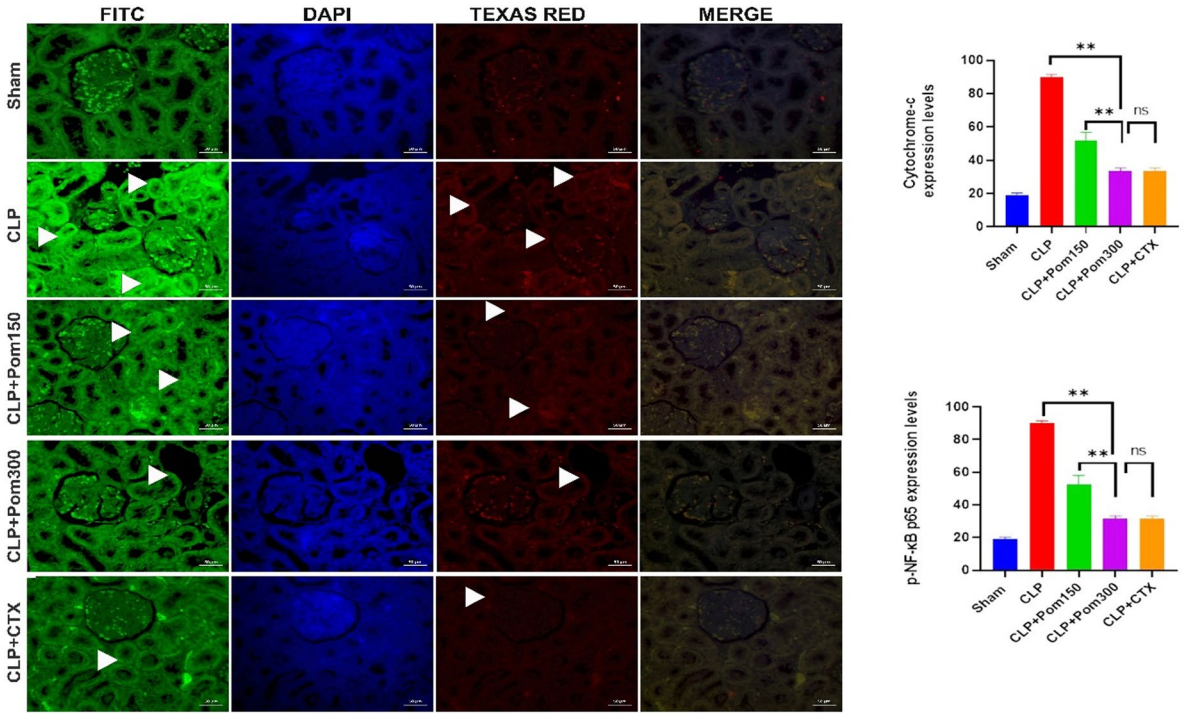

Fig. 13. Effect of pomiferin and CLP technique on cytochrome-c and p-NF-κB p65 expressions in kidney tissues. Cytochrome-c expressions (arrowheads) (FITC); p-NF-κB p65 expressions (arrowheads) (TEXAS RED). CLP: Cecal ligation and puncture, Pom: Pomiferin, CTX: Ceftriaxone. Findings are expressed as mean ± SD. **($p = 0.0028$). ns: Nonsignificant difference ($p > 0.05$).

NF-κB p65, and p-NF-κB p65. Specifically, TLR4, a transmembrane protein of the TLR family located on the cell surface, recognizes trace amounts of lipopolysaccharide (LPS) during sepsis, triggering a chain of protein reactions[32] including activation of the inhibitor of NF-κB kinase (IKK) complex, phosphorylation of the IκB/NF-κB p65 complex, and translocation of p-NF-κB p65 from the cytoplasm to the nucleus. This increases nuclear NF-κB accumulation and cytokine production, initiating the inflammatory response[30,31,33]. The increased expression of TLR4, NF-κB p65, and p-NF-κB p65 in liver and kidney tissues observed here indicates that the CLP technique activated this pathway, promoting phosphorylation of NF-κB p65, enhancing NF-κB transcription, and thereby aggravating inflammation. Previous studies have also shown that CLP activates the TLR4/NF-κB pathway in the liver[34] and kidney[35]. Thus, the NF-κB activation series represents a therapeutic target for suppressing inflammation during SA-ALI and SA-AKI. Pomiferin, particularly at 300 mg/kg, exerted anti-inflammatory effects by inhibiting this cascade (TLR4, NF-κB p65, and p-NF-κB p65) and suppressing NF-κB p65 phosphorylation in hepatic and renal tissues, suggesting a clear protective effect against sepsis-induced inflammatory damage. To our knowledge, only one in vitro study has reported anti-inflammatory effects of pomiferin via NF-κB inhibition; there, the authors showed that it reduced IκBα and p65 phosphorylation in LPS-treated BV2 cells[36]. Tang et al.[17]. further demonstrated that pomiferin attenuated LPS-induced inflammation in an in vivo ARDS model by blocking the AKT/Foxo1 signaling pathway. Osajin also showed anti-inflammatory effects in SA-ALI and SA-AKI models, but by suppressing IL-33, which triggers the inflammatory process during sepsis[20,21].

Under normal conditions, ROS perform essential cellular functions. In sepsis, however, their levels rise excessively, depleting the cellular antioxidant system and resulting in oxidative stress. During oxidative stress, cellular components, particularly the membrane, are highly susceptible to ROS attack, leading to increased LPO and further damage. ROS injury extends beyond lipids, proteins, and nucleic acids; ROS also worsen inflammation by stimulating the NF-κB activation series through phosphorylation of the IκB/NF-κB p65 complex by IKK, thereby activating NF-κB and promoting its nuclear translocation[37]. Reducing oxidative stress can therefore also diminish inflammation. The elevated LPO levels and collapse of antioxidant defenses in the CLP group confirm the development of oxidative stress in liver and kidney tissues. In contrast, pomiferin suppressed LPO, restored antioxidant capacity, and reestablished cellular homeostasis. This antioxidant activity is linked to its chemical structure, which contains two adjacent hydroxyl groups in the B ring (catechol group), conferring strong hydrogen-donating ability. This property is comparable to that of established antioxidants such as ascorbic acid and trolox[38]. In BV2 cells treated with LPS, pomiferin reduced ROS and nitric oxide production via activation of Akt and Nrf2 pathways[36]. Similarly, osajin, another *M. pomifera* isoflavone, reduced LPO and enhanced antioxidant defenses in liver and kidney tissues in SA-ALI and SA-AKI models[20,21].

DNA, like other cellular components, is vulnerable to ROS attack. Accordingly, 8-OHdG expression was measured to assess oxidative DNA damage in liver and kidney tissues. Moreover, mitochondrial DNA is more

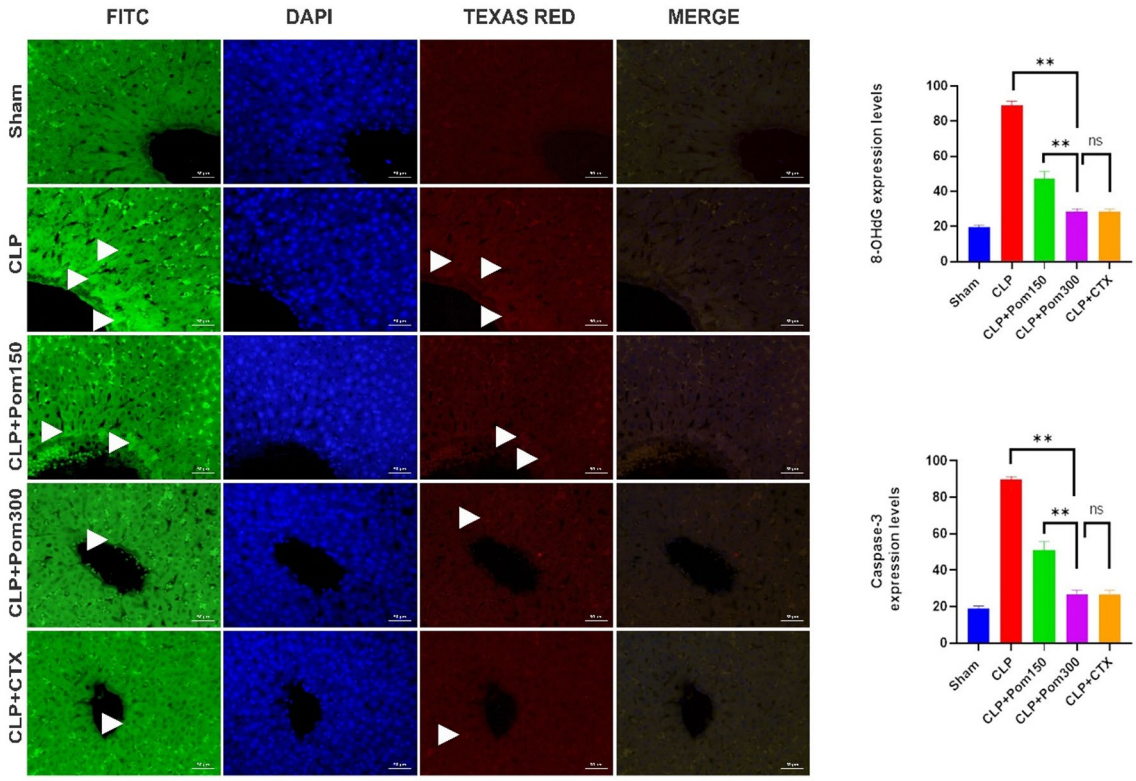

Fig. 14. Effect of pomiferin and CLP technique on 8-OHdG and caspase-3 expressions in liver tissues. 8-OHdG expressions (arrowheads) (FITC); caspase-3 expressions (arrowheads) (TEXAS RED). CLP: Cecal ligation and puncture, Pom: Pomiferin, CTX: Ceftriaxone. Findings are expressed as mean ± SD. For 8-OHdG **($p = 0.0028$), For caspase-3 **($p = 0.0022$). ns: Nonsignificant difference ($p > 0.05$).

susceptible to damage than nuclear DNA because it lacks histones and resides in a ROS-rich environment generated by the electron transport chain[39]. 8-OHdG is formed when hydroxyl radicals attack the guanine nucleobase at the C8 position[40]. We believe that persistent ROS overproduction and the observed antioxidant system deficiency in the CLP group caused mitochondrial and DNA damage, explaining the elevated 8-OHdG expression in hepatic and renal tissues. In addition to its use as a marker of DNA damage, serum 8-OHdG has been proposed as a biomarker for predicting mortality in sepsis patients[41]. Elevated DNA damage has been reported in critically ill septic patients[42]. Furthermore, 8-OHdG contributes to apoptosis by stimulating caspases and p53[43,44]. In severe sepsis, relationships have been observed between ROS levels, DNA damage, apoptosis, and necrosis[45]. Therefore, targeting 8-OHdG is a potential strategy to inhibit apoptosis signaling pathways. In this study, pomiferin's potent antioxidant activity suppressed DNA damage and reduced 8-OHdG levels in liver and kidney tissues, suggesting a protective role for this isoflavone in preserving genetic material in sepsis and disrupting the apoptosis cascade. In this context, osajin also demonstrated a clear ability to protect genetic material from damage during sepsis by reducing the level of 8-OHdG in kidney and brain tissues[21,46].

Cytochrome-c, a small hemeprotein located in the mitochondrial inner membrane, contributes to cellular energy production through electron transport[47]. Oxidative stress damages the mitochondrial membrane, causing cytochrome-c release into the cytoplasm. This initiates apoptosis by binding apoptosis-activating factor-1 (Apaf-1) and procaspase-9 to form the apoptosome, which activates a cascade of caspases including caspase-9, caspase-7, and caspase-3[43,47]. Caspase-3 then translocates to the nucleus, where it executes apoptosis via DNA fragmentation and chromatin condensation[48]. Thus, cytochrome-c expression serves as an indicator of mitochondrial membrane integrity and cellular shifts favoring apoptosis, which can also be tracked by caspase-3 expression. Elevated cytochrome-c and caspase-3 expression in the CLP group indicate severe mitochondrial damage and apoptosis in hepatic and renal tissues. Pomiferin, especially at 300 mg/kg, preserved mitochondrial integrity and exerted anti-apoptotic effects. In a recent study, pomiferin at this dose protected against nickel-induced hepatic injury by attenuating LPO, NF-κB, 8-OHdG, and caspase-3, while enhancing the antioxidant defense system in liver tissue[18]. Anti-apoptotic effects have also been reported for osajin in a rat model of sepsis by suppressing the expression of caspase-3[20,21,46] and Bcl-2-associated×protein (Bax)[46] in different rat tissues.

The necrosis observed in kidney and liver tissues in the CLP group could be attributed to exposure of these tissues to hypoxia due to the inflammation and overproduction of ROS attacking cell membranes[21]. Cell membrane damage is the first stage in the occurrence of necrosis[49]. The interstitial nephritis observed in CLP group could be attributed to the migration of leukocytes into the interstitial spaces[50]. Additionally, the influx of certain types of leukocytes to the injury site, with the aim of clearance of apoptotic and necrotic cells, exacerbates

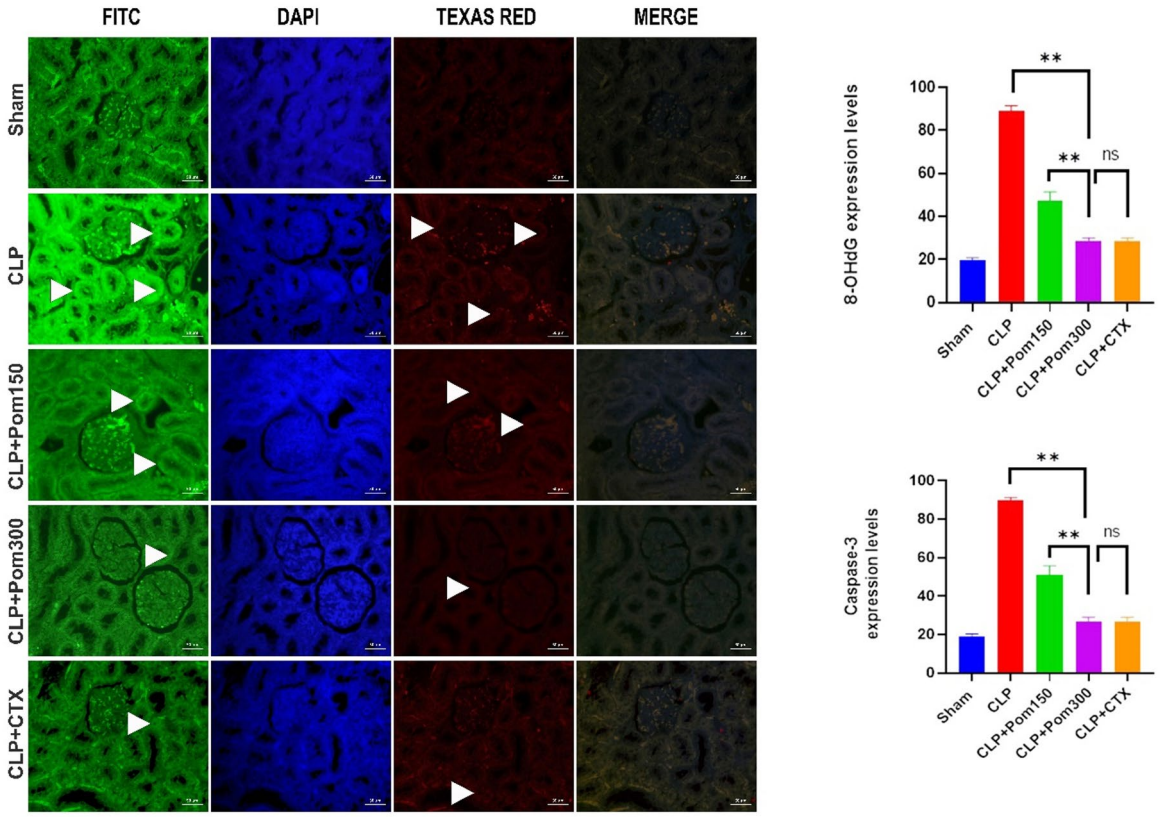

Fig. 15. Effect of pomiferin and CLP technique on 8-OHdG and caspase-3 expressions in kidney tissues. 8-OHdG expressions (arrowheads) (FITC); caspase-3 expressions (arrowheads) (TEXAS RED). CLP: Cecal ligation and puncture, Pom: Pomiferin, CTX: Ceftriaxone. Findings are expressed as mean ± SD. For 8-OHdG **($p = 0.0028$), For caspase-3 **($p = 0.0022$). ns: Nonsignificant difference ($p > 0.05$).

the inflammation[21]. Pomiferin at a dose of 300 mg/kg reversed these histopathological changes via its efficacy as a ROS scavenger and natural inhibitor of the inflammatory process. Likewise, osajin, another *M. pomifera* isoflavone, alleviated changes in hepatic and renal histopathology in SA-ALI and SA-AKI models[20,21]. Another study by Deniz et al.. demonstrated that administration of pomiferin, at a dose of 300 mg/kg, diminished histopathologic evidence in rat model of hepatotoxicity induced by nickel[18].

Overall, in this study the observed improvements in biochemical, immunohistochemical, and immunofluorescent parameters were mirrored by better histological integrity in the liver and kidney. Figure 16 illustrates the proposed pathophysiology of SA-ALI and SA-AKI and the pathways targeted by pomiferin.

The assessment of IKK, IκB, inflammatory cytokines, Bax, apoptosome, and caspase-9 expressions in hepatic and renal tissues would have expanded the results. Despite these limitations, we inferred the therapeutic effects of pomiferin against SA-ALI and SA-AKI. However, these parameters will be measured in future investigation.

Conclusion

This study confirms the role of the NF-κB activation series, oxidative stress, and cytochrome-c in the pathophysiology of SA-ALI and SA-AKI. Moreover, it provides evidence that pomiferin's therapeutic effects are linked to its ability to scavenge ROS, preserve the cellular antioxidant system, and suppress the progression of inflammatory processes. Specifically, pomiferin was found to exert protective effects against SA-ALI and SA-AKI by suppressing the NF-κB activation series, oxidative stress, and cytochrome-c in hepatic and renal tissues, supporting its potential as a proposed therapeutic candidate in the clinical management of sepsis patients with these complications after conducting further investigations in this regard.

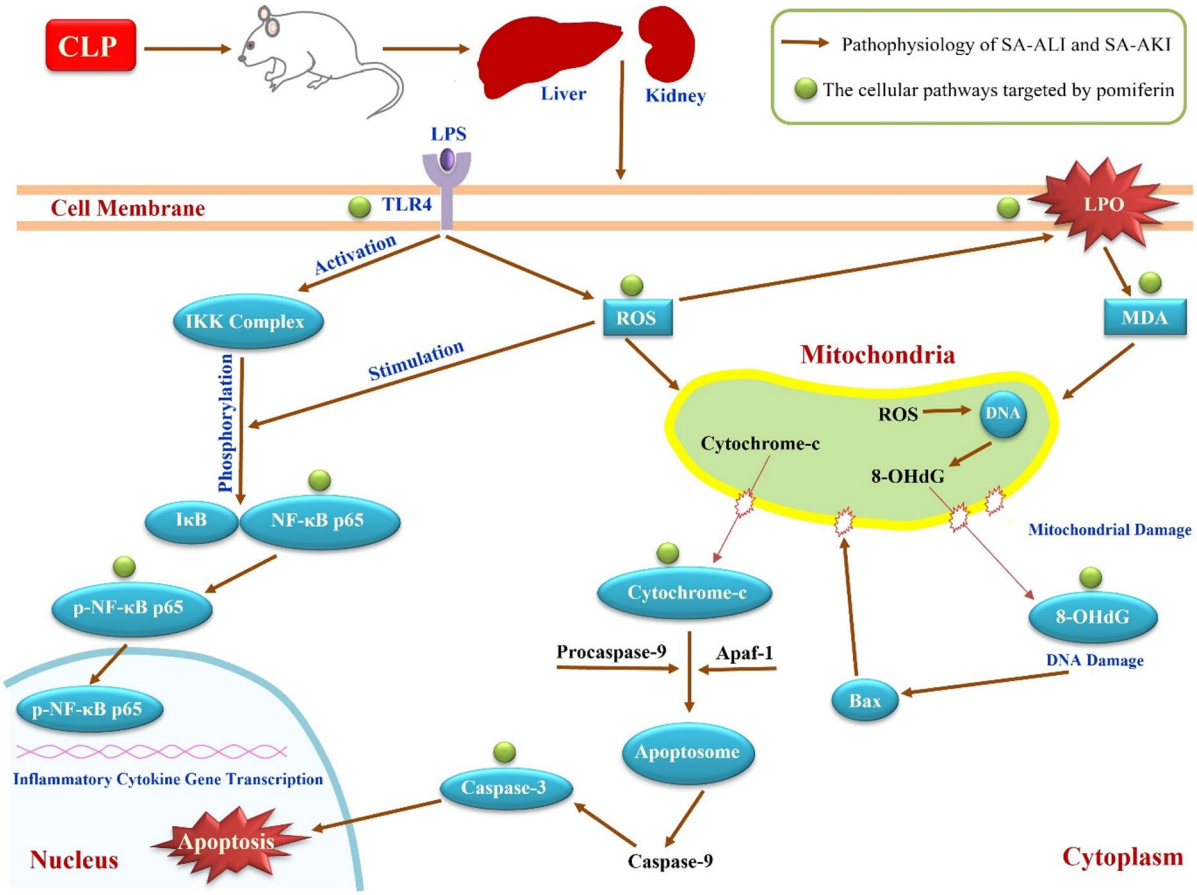

Fig. 16. The proposed pathophysiology of SA-ALI and SA-AKI, and the cellular pathways targeted by pomiferin. TLR4, located on the cell surface, recognizes LPS during sepsis, triggering a chain of NF-κB and ROS production. ROS promote inflammation by activating the NF-κB pathway. ROS overproduction also stimulates oxidative stress. This interplay between inflammation and oxidative stress in sepsis, causing cytochrome-c activation and ultimately apoptosis. Pomiferin exerts protective effects against SA-ALI and SA-AKI by suppressing the NF-κB activation series, oxidative stress, and cytochrome-c. CLP: Cecal ligation and puncture, SA-ALI: Sepsis-associated acute liver injury, SA-AKI: Sepsis-associated acute kidney injury.

Data availability

The data of this study are available in this article. Other data of this study are available from the corresponding author upon reasonable request.

Received: 28 August 2025; Accepted: 17 March 2026
Published online: 21 March 2026

References

1. Zhou, Y., Yu, Z. & Lu, Y. To explore the influencing factors of clinical failure of anti-tumor necrosis factor-α (TNF-α) therapy in sepsis. *Life Sci.* **369**, 123556. https://doi.org/10.1016/j.lfs.2025.123556 (2025).
2. Borges, A. & Bento, L. Organ crosstalk and dysfunction in sepsis. *Ann. Intensive Care* **14**, 147. https://doi.org/10.1186/s13613-024-01377-0 (2024).
3. Kumar, N. R., Balraj, T. A., Kempegowda, S. N. & Prashant, A. Multidrug-resistant sepsis: A critical healthcare challenge. *Antibiotics* **13**(1), 46. https://doi.org/10.3390/antibiotics13010046 (2024).
4. Van den Berg, M., Van Beuningen, F. E., Ter Maaten, J. C. & Bouma, H. R. Hospital-related costs of sepsis around the world: A systematic review exploring the economic burden of sepsis. *J. Crit. Care* **71**, 154096. https://doi.org/10.1016/j.jcrc.2022.154096 (2022).
5. Li, J., Lu, Y. & Lin, G. Blocking cGAS/STING signaling protects against sepsis-associated acute liver injury. *Int. Immunopharmacol.* **113**, 109276. https://doi.org/10.1016/j.intimp.2022.109276 (2022).
6. Gong, R. et al. Piplartine alleviates sepsis-induced acute kidney injury by inhibiting TSPO-mediated macrophage pyroptosis. *Biochimica et Biophysica Acta (BBA) - Molecular Basis of Disease* **1871**(3), 167687. https://doi.org/10.1016/j.bbadis.2025.167687 (2025).
7. Guo, Y., Guo, W., Chen, H., Sun, J. & Yin, Y. Mechanisms of sepsis-induced acute liver injury: A comprehensive review. *Front. Cell. Infect. Microbiol.* **15**, 1504223. https://doi.org/10.3389/fcimb.2025.1504223 (2025).
8. Zarbock, A. et al. Sepsis-associated acute kidney injury: Consensus report of the 28th Acute Disease Quality Initiative workgroup. *Nat. Rev. Nephrol.* **19**, 401–17. https://doi.org/10.1038/s41581-023-00683-3 (2023).

9. Xu, X., Yang, T., An, J., Li, B. & Dou, Z. Liver injury in sepsis: Manifestations, mechanisms and emerging therapeutic strategies. *Front. Immunol.* **16**, 1575554. https://doi.org/10.3389/fimmu.2025.1575554 (2025).
10. Wu, Z. et al. Programmed cell death in sepsis associated acute kidney ınjury. *Front. Med.* **9**, 883028. https://doi.org/10.3389/fmed.2022.883028 (2022).
11. Liu, D., Li, L. & Li, Z. Anemonin inhibits sepsis-induced acute kidney injury via mitigating inflammation and oxidative stress. *Biotechnol. Appl. Biochem.* **70** (6), 1983–2001. https://doi.org/10.1002/bab.2504 (2023).
12. Gao, J. et al. Protective role of crocin against sepsis-induced injury in the liver, kidney and lungs via inhibition of p38 MAPK/NF-κB and Bax/Bcl-2 signalling pathways. *Pharm. Biol.* **60**(1), 543–52. https://doi.org/10.1080/13880209.2022.2042328 (2022).
13. Srdić, T. et al. From molecular mechanisms to clinical therapy: Understanding sepsis-induced multiple organ dysfunction. *Int. J. Mol. Sci.* **25**(14), 7770. https://doi.org/10.3390/ijms25147770 (2024).
14. Yu, Y. Y. et al. Self-developed NF-κB inhibitor 270 protects against LPS-induced acute kidney injury and lung injury through improving inflammation. *Biomed. Pharmacother.* **147**, 112615. https://doi.org/10.1016/j.biopha.2022.112615 (2022).
15. Filip, S. et al. Chemical composition and antimicrobial activity of Osage orange (Maclura pomifera) leaf extracts. *Arch. Pharm.* **354** (2), 2000195. https://doi.org/10.1002/ardp.202000195 (2021).
16. Bozkurt, İ et al. Investigation on the effects of pomiferin from *Maclura pomifera* on indomethacin-induced gastric ulcer: An experimental study in rats. *Med. Chem. Res.* **26**, 2048–56. https://doi.org/10.1007/s00044-017-1913-y (2017).
17. Tang, Z., Yang, Z., Feng, H., Zhou, X. & Mao, M. Attenuation of the severity of acute respiratory distress syndrome by Pomiferin through blocking inflammation and oxidative stress in an AKT/Foxo1 pathway-dependent manner. *Oxid. Med. Cell. Longev.* 5236908. https://doi.org/10.1155/2022/5236908 (2022).
18. Deniz, G. Y., Geyikoglu, F. & Altun, S. The regulatory effects of pomiferin dietary on nickel-induced hepatic injury in Sprague–Dawley rats; action mechanisms and signaling pathways. *Toxicol Mech Methods* **34**(5), 484–94. https://doi.org/10.1080/15376516.2023.2301667 (2024).
19. Zhao, Y., Sang, Y. & SunY, Wu, J. Pomiferin exerts antineuroinflammatory effects through activating Akt/Nrf2 pathway and ınhibiting NF- κ B pathway. *Mediators Inflamm.* 5824657. https://doi.org/10.1155/2022/5824657 (2022).
20. Alhilal, M. et al. Osajin from *Maclura pomifera* alleviates sepsis-induced liver injury in rats: Biochemical, histopathological and immunohistochemical estimation. *Journal of Taibah University for Science* **17**(1), 2201250. https://doi.org/10.1080/16583655.2023.2201250 (2023).
21. Alhilal, M. et al. Medicinal evaluation and molecular docking study of osajin as an anti-inflammatory, antioxidant, and antiapoptotic agent against sepsis-associated acute kidney injury in rats. *Ren Fail* **46**(2), 2379008. https://doi.org/10.1080/0886022X.2024.2379008 (2024).
22. Fujimura, N. et al. Effect of free radical scavengers on diaphragmatic contractility in septic peritonitis. *Am. J. Respir Crit. Care Med.* **162** (6), 2159–2165. https://doi.org/10.1164/ajrccm.162.6.9912144 (1999).
23. Moon, H. I. Effect of osajin and pomiferin on antidiabetic effects from normal and streptozotocin-induced diabetic rats. *Nat Prod Commun* **9**(12), 1723–24. https://doi.org/10.1177/1934578X1400901215 (2014).
24. Zaychenko, G. V. & Tatskiy, Y. O. Prostatoprotective effect of *Maclura pomifera* oil extract and the way it is implemented. *Medical Science of Ukraine (MSU)* **17**(1), 68–73. https://doi.org/10.32345/2664-4738.1.2021.09 (2021).
25. Keleş, O. N. et al. Protective effects of pomiferin isolated from *Maclura pomifera* on ischemia-reperfusion injury of rat ovary: Biochemical and histopathologic evaluation. *International Journal of Research in Medical Sciences* **11**(2), 433–41. https://doi.org/10.18203/2320-6012.ijrms20230010 (2023).
26. Ohkawa, H., Ohishi, N. & Yagi, K. Assay for lipid peroxides in animal tissues by thiobarbituric acid reaction. *Anal. Biochem.* **95** (2), 351–358. https://doi.org/10.1016/0003-2697(79)90738-3 (1979).
27. Sedlak, J. & Lindsay, R. H. Estimation of total, protein-bound, and nonprotein sulfhydryl groups in tissue with Ellman's reagent. *Anal. Biochem.* **25**, 192–205. https://doi.org/10.1016/0003-2697(68)90092-4 (1968).
28. Sun, Y., Oberley, L. W. & Li, Y. A simple method for clinical assay of superoxide dismutase. *Clin. Chem.* **34** (3), 497–500. https://doi.org/10.1093/clinchem/34.3.497 (1988).
29. Aebi, H. Catalase in vitro. *Methods Enzymol.* **105**(C), 121–6. https://doi.org/10.1016/S0076-6879(84)05016-3 (1984).
30. Tang, Y. et al. Dimethyl fumarate attenuates LPS induced septic acute kidney injury by suppression of NFκB p65 phosphorylation and macrophage activation. *Int. Immunopharmacol.* **102**, 108395. https://doi.org/10.1016/j.intimp.2021.108395 (2022).
31. Abraham, E. Nuclear factor – $_{\kappa}$B and its role in sepsis- Associated organ failure. *J. Infect. Dis.* **187**(Suppl 2), S364–S369. https://doi.org/10.1086/374750 (2003).
32. Kuzmich, N. N. et al. TLR4 signaling pathway modulators as potential therapeutics in inflammation and sepsis. *Vaccines* **5**(4), 34. https://doi.org/10.3390/vaccines5040034 (2017).
33. Zhang, H. et al. DHA-enriched phosphatidylserine ameliorates cyclophosphamide-induced liver injury via regulating the gut-liver axis. *Int. Immunopharmacol.* **140**, 112895. https://doi.org/10.1016/j.intimp.2024.112895 (2024).
34. Makled, M. N. et al. Pomegranate protects liver against cecal ligation and puncture-induced oxidative stress and inflammation in rats through TLR4/NF-κB pathway inhibition. *Environ. Toxicol. Pharmacol.* **43**, 182–92. https://doi.org/10.1016/j.etap.2016.03.011 (2016).
35. Senousy, S. R. et al. Alpha-chymotrypsin protects against acute lung, kidney, and liver injuries and increases survival in CLP-induced sepsis in rats through inhibition of TLR4/NF-κB pathway. *Drug Des. Devel. Ther.* **16**, 3023–39. https://doi.org/10.2147/DDDT.S370460 (2022).
36. Zhao, Y., Sang, Y., Sun, Y. & Wu, J. Pomiferin exerts antineuroinflammatory effects through activating Akt/Nrf2 pathway and inhibiting NF- κ B pathway. *Mediators Inflamm.* 5824657. https://doi.org/10.1155/2022/5824657 (2022).
37. Sul, O. J. & Ra, S. W. Quercetin prevents LPS-induced oxidative stress and inflammation by modulating NOX2/ROS/NF-kB in lung epithelial cells. *Molecules* **26**, 26:6949. https://doi.org/10.3390/molecules26226949 (2021).
38. Teixeira, J. G., Dias, C. B. & Teixeira, D. M. Electrochemical characterization and quantification of the strong antioxidant and antitumor agent pomiferin. *Electroanalysis* **21**(21), 2345–53. https://doi.org/10.1002/elan.200900178 (2009).
39. Ferreira, T. & Rodriguez, S. Mitochondrial DNA: Inherent complexities relevant to genetic analyses. *Genes* **15**(5), 617. https://doi.org/10.3390/genes15050617 (2024).
40. Yadav, V., Krishnan, A. & Vohora, D. Altered hallmarks of DNA double-strand breaks, oxidative DNA damage and cytogenotoxicity by piperlongumine in hippocampus and hepatocytes of rats intoxicated with cyclophosphamide. *Life Sci.* **316**, 121391. https://doi.org/10.1016/j.lfs.2023.121391 (2023).
41. Lorente, L. et al. Association between DNA and RNA oxidative damage and mortality in septic patients. *J. Crit. Care* **54**, 94–8. https://doi.org/10.1016/j.jcrc.2019.08.008 (2019).
42. Mihaljevic, O. et al. Oxidative stress and DNA damage in critically ill patients with sepsis. *Mutat. Res. Genet. Toxicol. Environ. Mutagen.* **889**, 503655. https://doi.org/10.1016/j.mrgentox.2023.503655 (2023).
43. O'Brien, M. A. & Kirby, R. Apoptosis: A review of pro-apoptotic and anti-apoptotic pathways and dysregulation in disease. *J. Vet. Emerg. Crit. Care* **18**(6), 572–85. https://doi.org/10.1111/j.1476-4431.2008.00363.x (2008).
44. Sifuentes-Franco, S., Padilla-Tejeda, D. E., Carrillo-Ibarra, S. & Miranda-Díaz, A. G. Oxidative stress, apoptosis, and mitochondrial function in diabetic nephropathy. *Int. J. Endocrinol.* 1875870. https://doi.org/10.1155/2018/1875870 (2018).
45. Bahar, I., Elay, G., Başkol, G., Sungur, M. & Donmez-Altuntas, H. Increased DNA damage and increased apoptosis and necrosis in patients with severe sepsis and septic shock. *J. Crit. Care.* **43**, 271–5. https://doi.org/10.1016/j.jcrc.2017.09.035 (2018).

46. Alhilal, M. et al. Osajin is a promising candidate for sepsis-induced brain damage via suppression of the 8-OHdG/Bax/Caspase-3 pathway in a rat model of sepsis. *J. Health Sci. Med.* **8**, 191–6. https://doi.org/10.32322/jhsm.1614590 (2025).
47. Eleftheriadis, T., Pissas, G., Liakopoulos, V. & Stefanidis, I. Cytochrome c as a potentially clinical useful marker of mitochondrial and cellular damage. *Front. Immunol.* **7**, 279. https://doi.org/10.3389/fimmu.2016.00279 (2016).
48. Mantzarlis, K., Tsolaki, V. & Zakynthinos, E. Role of oxidative stress and mitochondrial dysfunction in sepsis and potential therapies. *Oxid. Med. Cell. Longev.* 5985209. https://doi.org/10.1155/2017/5985209 (2017).
49. Oberholzer, C., Oberholzer, A., Clare-Salzler, M. & Moldawer, L. L. Apoptosis in sepsis: A new target for therapeutic exploration. *FASEB J.* **15**(6), 879–892. https://doi.org/10.1096/fsb2fj00058rev (2001).
50. Peerapornratana, S., Manrique-Caballero, C. L., Gómez, H. & Kellum, J. A. Acute kidney injury from sepsis: Current concepts, epidemiology, pathophysiology, prevention and treatment. *Kidney Int.* **96**(5), 1083–99. https://doi.org/10.1016/j.kint.2019.05.026 (2019).

Author contributions

Conceptualization, M.B.H., O.N.K., H.S.E. and M.A.; methodology, M.B.H., O.N.K., M.A., H.S.E. and S.Y.; validation, M.B.H., M.A., O.N.K., H.S.E., S.Y., S.A., E.D., M.K., T.K., E.A.S. and I.B.; formal analysis, M.A., H.S.E., S.Y. and E.D.; investigation, M.A., M.B.H., O.N.K., H.S.E., S.Y., S.A., E.D., M.K., T.K., E.A.S. and I.B.; writing—original draft preparation, M.A.; writing—review and editing, M.A., M.B.H., O.N.K., H.S.E., S.Y., S.A., E.D., M.K., T.K., E.A.S. and I.B.; visualization, M.A., M.B.H., O.N.K., H.S.E., S.Y., S.A., E.D., M.K., T.K., E.A.S. and I.B.; supervision, M.B.H.; project administration, M.B.H. All authors have read and agreed to the published version of the manuscript.

Funding

We thank Ataturk University (Erzurum, Turkey) for providing funding to this study (The project id 2015/300).

Declarations

Competing interests

The authors declare no competing interests.

Ethics approval

This study was approved by the Ethics Committee of Animal Experiments at Ataturk University, Erzurum, Turkey (Approval No. 134, Date. 01.09.2015).

Additional information

Correspondence and requests for materials should be addressed to M.A.

Reprints and permissions information is available at www.nature.com/reprints.

Publisher's note Springer Nature remains neutral with regard to jurisdictional claims in published maps and institutional affiliations.